Current Topics in Electrochemistry
Vol. 19, 2017

Original Communication

An insightful theoretical model of the performance behavior of a lithium-ion cell electrode

Sarwan S. Sandhu[1,*], Joseph P. Fellner[2] and Srikar P. Dudi[1]

[1]Department of Chemical and Materials Engineering, University of Dayton, Dayton, OH 45469;
[2]Air Force Research Laboratory, Wright-Patterson AFB, OH 45433-7251, USA.

ABSTRACT

A theoretical model of lithium-ion mass transport in a thin platelet-like active material particle of a composite electrode of a lithium-ion cell relative to the lithium-ion mass transport in the electrolyte was developed to provide insight into the performance behavior of the electrode. The developed formulation predicts the dimensionless transient lithium ion concentration profiles in the solid state active material particle, electrode-electrolyte interfacial current density, and g-moles of intercalatable lithium per g-mole of lithium-free electrode active material.

KEYWORDS: lithium-ion electrode, active material platelet-like particle, transient lithium-ion concentration profiles, interfacial current density, lithium-ion mass diffusivity.

1. INTRODUCTION

Examples of clean energy sources are geothermal energy, solar radiation, wind, and ocean water waves. In addition to the cleaner energy sources, efficient systems are needed to store electrical energy produced from these sources in excess of its demand. Rechargeable batteries are one example of an efficient electrical energy storage system. They provide portable stored chemical energy which is converted into electrical energy on demand with a high conversion efficiency in the absence of environmental harmful emissions. Among the various types of rechargeable batteries currently available, the lithium-ion-based batteries possess the highest energy density and are flexible in design. Rechargeable lithium-ion cells are one of the major components of portable computing and telecommunication systems [1].

Many cathode electrode materials have been developed and tested for their application in primary and secondary batteries; for example, $LiMn_2O_4$, $LiCoO_2$, $LiFePO_4$, $LiNi_{1/3}Mn_{1/3}Co_{1/3}O_2$, etc. High energy storage capacity materials based on phthalocyanines, such as iron phthalocyanine (FePc) and copper phthalocyanine (CuPc), are also currently being tested [2] as potential cathode active materials. Model development at the active material particle level [3], and with scale-up to the electrode level, is needed to help in the design and performance prediction of new lithium-ion batteries. It is also anticipated that fundamental modeling will aid in the faster development of any new types of active materials for lithium-ion batteries.

A high charge capacity lithium-ion cell cathode electrode is, in general, composed of an electrolyte dispersed among particles of an active solid state material in a certain particle size range. Active material particles are interconnected through an electronic conductor and a binder. Ideal particle geometrical shape for modeling purpose is rectangular (i.e. platelet-like), cylindrical or spherical. The ideal particle geometry-level modeling can be extended to a non-ideal particle shape through the application of shape factor, $f_{geom,\ shap}$, defined as: [(outer surface area/volume ratio of a particle of a non-geometrical shape) divided by (outer surface area/volume ratio of a particle of an ideal shape)].

*Corresponding author: ssandhu1@udayton.edu

After this, one can also account for the particle size distribution effect in the electrode design and performance equation set. Although a large body of literature [4-22] on the lithium-ion cell/battery modeling exists, the model presented in this short paper deals with transport of lithium ions *via* diffusion in a platelet-like active material particle which is thin and of relatively simple geometry. This theoretical task was undertaken to gain insight into the effect of lithium-ion diffusive transport in the electrode active material relative to that in the cell electrolyte on the performance behavior of a thin lithium-ion cell electrode.

2. MODEL FORMULATION

Figure 1 shows a sketch of a very thin platelet-like particle in contact with an electrolyte in a composite material electrode. Here, the particle surface areas along the edges AD and BC are assumed to be negligibly small relative to the surface areas along the edges AB and CD in contact with the electrolyte.

In general, lithium ions in an electrolyte can move under the influence of spatial gradients of lithium-ion chemical (or concentration) and electric potentials. Similarly, transport of lithium ions in a solid active material of an electrode can take place under the effect of lithium-ion spatial concentration gradient as well as electric potential gradient. Lithium-ion transport across the interface between the electrode active material and the electrolyte

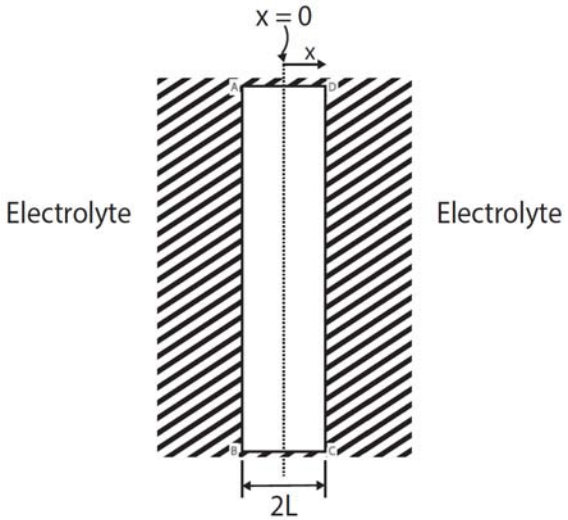

Figure 1. A thin platelet-like particle in contact with an electrolyte.

in contact with it takes place through the 'electrochemical' process of charge separation/ combination. Net transport of lithium ions in the electrode active material can be modeled using the effective lithium diffusivity concept accounting for both the spatial concentration and electric potential gradient effects on lithium ion transport. Similarly, transport of lithium ions in the electrolyte *via* both spatial concentration and electric potential gradients can be simulated by application of effective mass transfer coefficient. Resistance to transport of electrons in an electronic conductor of the composite electrode is negligibly small. Furthermore, it is currently known that the lithium ion diffusion is the dominant limiting mechanism for lithium ion transport in a composite electrode active material, e.g., $LiMn_2O_4$, $LiNi_{1/3}Mn_{1/3}$ $Co_{1/3}O_2$, $LiFePO_4$, V_2O_5, *FePc* (iron phthalocyanine), copper phthalocyanine (CuPc), etc., provided the ionic conductance in the electrolyte is equal to or greater than 1 mS cm^{-1} [2, 3]. It is here assumed that the lithium ion mass transfer out of/into the electrode solid active material relative to its mass transfer in the electrolyte is controlled by its diffusion in the active material solid phase; the electrochemical process of interaction between electrons and ions being relatively much faster. Transport of lithium ions in the solid active material, thin rectangular particle, shown in Figure 1, is described by the following partial differential equation (PDE) [23]:

$$\frac{\partial C}{\partial t} = \frac{\partial}{\partial x}\left(D_{eff} \frac{\partial C}{\partial x} \right) \tag{1}$$

D_{eff} is proposed to be concentration dependent [2], and therefore, it is a function of x. In the absence of availability of practical, experimentally based correlation showing the dependence of D_{eff} on the intercalated lithium ion concentration in the active material at constant temperature and pressure conditions, D_{eff} is, here, assumed constant. Eq. (1) then becomes:

$$\frac{\partial C}{\partial t} = D_{eff} \frac{\partial^2 C}{\partial x^2} \tag{2}$$

In this case, the initial condition and the two boundary conditions used to solve Eq. (2) are, respectively:

$$t \le 0, \quad 0 \le x \le L, \quad C = C_{max} f(x) \tag{3}$$

$$t > 0, \quad x = 0, \quad \frac{\partial C}{\partial x} = 0 \tag{4}$$

$$t > 0, \quad x = L, \quad \left(-D_{eff} \left. \frac{\partial C}{\partial x} \right|_{x=L^-} \right) = k_{eff,\,electro} \left(C_{electro}\big|_{x=L^+} - C^b_{electro} \right) = k_{eff,\,electro} \left(\frac{C\big|_{x=L^-}}{\alpha} - C^b_{electro} \right) \tag{5}$$

Equation (5) states that the lithium-ion molar flux to the $x = L$ interface between the active material and the electrolyte is equal to the molar flux of lithium ions from the interface into the electrolyte. In Eq. (5), α is a constant such that $C_{electro}\big|_{x=L^+} = \frac{C|_{x=L^-}}{\alpha}$; $C|_{x=L^-}$ = lithium ion concentration on the active material side at the interface; $C^b_{electro}$ = lithium ion molar concentration in the bulk electrolyte; and $k_{eff,\,electro}$ = effective lithium ion mass transfer coefficient for lithium ion mass transport in the concentration boundary layer present around the active material particle. In Eq. (3), $f(x)$ = dimensionless initial lithium concentration profile in the solid electrode active material particle; noting that for the uniform initial concentration profile, $f(x) = 1$.

By defining y as given below,

$$y = C - \alpha C^b_{electro} \tag{6}$$

Eq. (2) with the initial and boundary conditions given by Eq. (3)-(5) were transformed into the following form:

$$\frac{\partial y}{\partial t} = D_{eff} \frac{\partial^2 y}{\partial x^2} \tag{7}$$

$$t \le 0, \quad 0 \le x \le L; \quad y = C_{max} \left(f(x) - \frac{\alpha C^b_{electro}}{C_{max}} \right) \tag{8}$$

$$t > 0, \quad x = 0, \quad \frac{\partial y}{\partial x} = 0 \tag{9}$$

$$t > 0, \quad x = L, \quad \frac{\partial y}{\partial x} = -\beta y \tag{10}$$

where

$$\beta = \frac{k_{eff,\,electro}}{\alpha D_{eff}} \tag{11}$$

The mathematical method of separation of variables [24, 25] was used to solve Eq. (7) using the initial and boundary conditions Eq. (8) through (10). The resulting solution was transformed into the dimensionless form as given below:

$$C^d(\xi,\tau) = \frac{C(\xi,\tau) - \alpha C^b_{electro}}{C_{max}} = 2\sum_{n=1}^{n=\infty} \left[\left(\frac{\delta_n \int_0^1 f(\xi)\cos(\delta_n \xi)\,d\xi - (\alpha r)\sin\delta_n}{\delta_n + \sin\delta_n \cos\delta_n} \right) \cos(\delta_n \xi) e^{-\delta_n^2 \tau} \right] \tag{12}$$

where, the dimensionless time for lithium ion diffusion in the solid electrode active material, $\tau = \frac{D_{eff} t}{L^2}$; dimensionless distance, $\xi = \frac{x}{L}$, L = half thickness of the thin platelet-like active material particle; r = (ratio of the lithium ion concentration in the bulk electrolyte to the maximum lithium ion concentration in the electrode active material, e.g., in copper phthalocyanine= $\frac{C^b_{electro}}{C_{max}}$). Values of the parameter δ_n; $n = 1, 2, \ldots, n, \ldots, \infty$ for use in Eq. (12) are obtained from $\delta_n \tan\delta_n = \left(\frac{Lk_{eff,\,electro}}{\alpha D_{eff}} = c \right)$; the values of the first six roots of this algebraic equation are given in the reference [26]. The dimensionless group, $\left(\frac{Lk_{eff,\,electro}}{\alpha D_{eff}} = c \right)$, is a measure of the ratio of the lithium ion flux in the electrolyte to the lithium ion flux in a solid electrode active material particle.

The transient lithium concentrations at the active material particle central plane, $\xi = \frac{x}{L} = 0$, and at $\xi = \frac{x}{L} = 1$, on the active material particle side at the interface between the particle and the electrode electrolyte, are obtained by inserting $\xi = 0$ and $\xi = 1$, respectively, into Eq. (12).

$$\frac{C(\xi=0,\tau)-\alpha C^{b}_{electro}}{C_{max}} = 2\sum_{n=1}^{n=\infty}\left[\left(\frac{\delta_n\int_0^1 f(\xi)\cos(\delta_n\xi)d\xi-(\alpha r)\sin\delta_n}{\delta_n+\sin\delta_n\cos\delta_n}\right)e^{-\delta_n^2\tau}\right] \tag{13}$$

$$\frac{C(\xi=1,\tau)-\alpha C^{b}_{electro}}{C_{max}} = 2\sum_{n=1}^{n=\infty}\left[\left(\frac{\delta_n\int_0^1 f(\xi)\cos(\delta_n\xi)d\xi-(\alpha r)\sin\delta_n}{\delta_n+\sin\delta_n\cos\delta_n}\right)\cos(\delta_n)e^{-\delta_n^2\tau}\right] \tag{14}$$

From Eq. (12), $\left(\frac{\partial C}{\partial \xi}\right)\Big|_{\xi=\frac{x}{L}=1}$ was obtained and using the lithium molar flux from the solid active material particle interior to its interface with the electrolyte phase, $\dot{N}_{Li^+} = -D_{eff}\left(\frac{\partial C}{\partial x}\Big|_{\xi=\frac{x}{L}=1}\right)$, the following expression in dimensionless form was obtained:

$$\frac{\dot{N}_{Li^+}L}{D_{eff}C_{max}} = \frac{i_s L}{FD_{eff}C_{max}} = 2\sum_{n=1}^{n=\infty}\left\{\left(\frac{\delta_n\int_0^1 f(\xi)\cos(\delta_n\xi)d\xi-(\alpha r)\sin\delta_n}{\delta_n+\sin\delta_n\cos\delta_n}\right)\delta_n\sin(\delta_n)e^{-\delta_n^2\tau}\right\} \tag{15}$$

where i_s = interfacial current density, [A cm^{-2}], and F = Faraday constant = 96485 [C mol^{-1}].

Equation (15) shows that the lithium-ion molar flux from the interior of the active material particle to the electrolyte-active material interface, N_{Li^+}, or the interfacial current density, i_s, decreases as the dimensionless time, τ increases with lithium de-intercalation.

Initial amount of lithium in the electrode active material [g-mole of Li per gm of the intercalated lithium free active material] is given by:

$$n_{Li,\,ini} = \left(\frac{C_{Li,\,ini}}{\rho_{active\ material}}\right) = \frac{X_{ini}\left(\frac{\rho_{active\ material}}{M_{active\ material}}\right)}{\rho_{active\ material}} = \frac{X_{ini}}{M_{active\ material}} \tag{16}$$

If S_g is the effective lithium-ion transfer electrolyte-active material interfacial area per gm of the intercalated lithium free active material, the molar rate per gm of the active material, at which lithium ions are vacating the active material channels at any time [e.g., (g-moles of Li^+) per (gm of active material-time)], is given by

$$\dot{N}_{Li^+\ per\ gm} = \dot{N}_{Li^+}S_g \tag{17}$$

Depletion of the lithium amount in the active material particle in the time interval, from t to (t + dt) is given by:

$$dn_{Li^+} = -\dot{N}_{Li-per\ gm}dt = -\dot{N}_{Li}S_g dt \tag{18}$$

From $\tau = \frac{D_{eff}t}{L^2}$; $t = \left(\frac{L^2}{D_{eff}}\right)\tau$; therefore, $dt = \left(\frac{L^2}{D_{eff}}d\tau\right)$; inserting for dt into Eq. (18) leads to:

$$dn_{Li^+} = -\left(\frac{S_g L^2}{D_{eff}}\right)\dot{N}_{Li^+}d\tau \tag{19}$$

Inserting the expression for $\dot{N}_{Li^+}$ from Eq. (15) into Eq. (19), integrating the resultant expression from 'τ'= 0 to 'τ'= τ; correspondingly, from 'n_{Li+}'= $n_{Li^+,\,ini}$ to 'n_{Li+}'= n_{Li^+}, and simplifying leads to:

$$\left(\frac{n_{Li^+,ini}-n_{Li^+}}{S_g L C_{max}}\right)=2\sum_{n=1}^{n=\infty}\left\{\left(\frac{\delta_n\int_0^1 f(\xi)\cos(\delta_n\xi)d\xi-(\alpha r)\sin\delta_n}{\delta_n+\sin\delta_n\cos\delta_n}\right)\frac{\sin(\delta_n)}{\delta_n}\left(1-e^{-\delta_n^2\tau}\right)\right\} \tag{20}$$

where,

$$C_{max}=X_{max}\left(\frac{\rho_{\text{active material}}}{M_{\text{active material}}}\right) \tag{21}$$

X_{max} is the maximum or theoretical g-moles of lithium which can be intercalated in the electrode active material per g-mole of the intercalated lithium-free active material. Equation (20) represents, at any dimensionless time τ, the g-moles of lithium per gram active material which have left the thin platelet-like active material particle divided by the maximum g-moles of lithium which can be accommodated in the active material per gram of active material. Equation (20) can be expressed as

$$\left(\frac{n_{Li^+}}{n_{Li^+,ini}}\right)=1-\left(\frac{S_g L C_{max}}{n_{Li^+,ini}}\right)\left[2\sum_{n=1}^{n=\infty}\left\{\left(\frac{\delta_n\int_0^1 f(\xi)\cos(\delta_n\xi)d\xi-(\alpha r)\sin\delta_n}{\delta_n+\sin\delta_n\cos\delta_n}\right)\frac{\sin(\delta_n)}{\delta_n}\left(1-e^{-\delta_n^2\tau}\right)\right\}\right] \tag{22}$$

Equation (22) expresses the fraction of stored lithium or charge still in the electrode active material at any time, τ, when lithium is de-intercalating the electrode active material.

From Eq. (15), the active material-electrolyte interfacial current density is

$$i_s=\left(\frac{2FD_{eff}C_{max}}{L}\right)\sum_{n=1}^{n=\infty}\left\{\left(\frac{\delta_n\int_0^1 f(\xi)\cos(\delta_n\xi)d\xi-(\alpha r)\sin\delta_n}{\delta_n+\sin\delta_n\cos\delta_n}\right)\delta_n\sin(\delta_n)e^{-\delta_n^2\tau}\right\} \tag{23}$$

Assuming quasi-isotropic transport of lithium in the electrode active material as well as the isotropic charge transfer process at the electrode active material-electrolyte interface, the electrode current per unit mass of the active material is given as

$$i_{s-m}=i_s S_g \tag{24}$$

Under the ideal condition of uniform distribution of $i_{s\text{-}m}$ in a composite electrode, the total current associated with lithium ions leaving the electrode active material is given by

$$I_{out,electrode}=i_{s-m}m_{electrode}=i_s S_g m_{electrode} \tag{25}$$

Inserting i_s from Eq. (23) into Eq. (25) leads to:

$$\left(\frac{I_{out,electrode}L}{FD_{eff}C_{max}S_g m_{electrode}}\right)=2\sum_{n=1}^{n=\infty}\left\{\left(\frac{\delta_n\int_0^1 f(\xi)\cos(\delta_n\xi)d\xi-(\alpha r)\sin\delta_n}{\delta_n+\sin\delta_n\cos\delta_n}\right)\delta_n\sin(\delta_n)e^{-\delta_n^2\tau}\right\} \tag{26}$$

$$\left(\begin{array}{l}\text{g-moles of lithium ions in the solid}\\ \text{active material per gram of it at any time}\\ \hline \text{g-moles of lithium ions in the active}\\ \text{material per gram of it at the initial time}\end{array}\right) = \frac{n_{Li^+}}{n_{Li^+,\,ini}} = \frac{\left(\dfrac{X}{M_{active\ material}}\right)}{\left(\dfrac{X_{ini}}{M_{active\ material}}\right)} = \frac{X}{X_{ini}} \tag{27}$$

$$n_{Li^+,\,ini} = \left(\frac{X_{ini}}{M_{active\ material}}\right) \tag{28}$$

and

$$C_{max} M_{active\ material} = \left(X_{max}\frac{\rho_{active\ material}}{M_{active\ material}}\right) M_{active\ material} = X_{max}\rho_{active\ material} \tag{29}$$

where X is the g-moles of lithium in the electrode active material per g-mole of the intercalated lithium-free active material at time τ. Also, X_{max} is the maximum or theoretical g-moles of lithium which can be intercalated in the active material of the electrode per g-mole of the intercalated lithium-free active material. Using the information provided in Eq. (27), (28), and (29), Eq. (22) can be expressed as

$$\left(\frac{X}{X_{ini}}\right) = 1 - 2\left(\left(S_g \rho_{active\ material} L\right)\left(\frac{X_{max}}{X_{ini}}\right)\right)\times \left[\sum_{n=1}^{n=\infty}\left\{\left(\frac{\delta_n \int_0^1 f(\xi)\cos(\delta_n \xi)d\xi - (\alpha r)\sin\delta_n}{\delta_n + \sin\delta_n \cos\delta_n}\right)\frac{\sin(\delta_n)}{\delta_n}\left(1 - e^{-\delta_n^2 \tau}\right)\right\}\right] \tag{30}$$

Equations (26) and (30) can be used to predict $I_{out,\,electrode}$ (electrode current) and $\left(\dfrac{X}{X_{ini}}\right)$, respectively, at any time τ. For a given electrode material and its design (controlling $\rho_{active\ material}$, S_g, L, etc.), X can be predicted using Eq. (30) at any time, t; and hence, at any τ, provided $D_{eff} = D_{eff}(X)$ at time 't' is known. If $D_{eff}(X)$ is not known, measured experimental data on $I_{out,\,electrode}$ versus time can be used to develop $D_{eff}(X)$ versus t or τ relation. One should solve Eq. (26) by trial-error procedure at each measured $I_{out,\,electrode}$ current at each t so that D_{eff} at that time, t, or τ when used on the right side of Eq. (26) is very close to the left side of this equation at that time. Also, one can calculate X at each τ using Eq. (30). Thus, one can develop the information on D_{eff} vs. X at each τ value. Predicted values of X as a function of t or τ can be used to calculate the thermodynamic properties as a function of X or τ as suggested in Ref. [3]. Also, D_{eff} vs. X data can be used to develop a correlation suggested in Eq. (6) of Ref. [2].

For the lithium ion diffusion in the solid-state electrode active material as the dominant charge/discharge controlling process, one can predict i_s from Eq. (23) at any time. Then, using the Butler-Volmer-type electrokinetic equation for the charge transfer at the active material-electrolyte interface, one can predict the voltage loss associated with the charge transfer process. Also, corresponding to the $I_{out,\,electrode}$ current predicted by Eq. (26), one should be able to estimate the ohmic-type voltage loss in the composite electrode if the information on the effective ionic conductance of the electrolyte in the composite electrode is available. Similarly, with the knowledge of effective electronic conductance,

ohmic voltage loss due to the electron transport in the composite electrode can be estimated. Thus, an estimate of the total voltage loss corresponding to the electrode current, $I_{out,\ electrode}$, can be predicted for its eventual application in the determination of actual cell voltage corresponding to $I_{out,\ electrode}$ controlled by the lithium-ion diffusion in the solid active material of a composite electrode relative to the lithium ion mass transfer in the electrolyte.

Under the assumption of uniform distribution of lithium in the platelet-type active material particle, i.e $f(\xi) = f\left(\frac{x}{L}\right) = 1$, the above presented formulation led to the following set of analytical formulas

$$C^d(\xi,\tau) = \frac{C(\xi,\tau) - \alpha C^b_{electro}}{C_{max}(1-\alpha r)} = 4\sum_{n=1}^{n=\infty}\left[\left(\frac{\sin\delta_n \cos(\delta_n \xi)}{2\delta_n + \sin(2\delta_n)}\right)e^{-\delta_n^2 \tau}\right] \tag{31}$$

$$\frac{C(\xi=0,\tau) - \alpha C^b_{electro}}{C_{max}(1-\alpha r)} = 4\sum_{n=1}^{n=\infty}\left[\frac{\sin\delta_n}{2\delta_n + \sin(2\delta_n)}e^{-\delta_n^2 \tau}\right] \tag{32}$$

$$\frac{C(\xi=1,\tau) - \alpha C^b_{electro}}{C_{max}(1-\alpha r)} = 2\sum_{n=1}^{n=\infty}\left[\frac{\sin(2\delta_n)}{2\delta_n + \sin(2\delta_n)}e^{-\delta_n^2 \tau}\right] \tag{33}$$

$$\frac{\dot{N}_{Li^+} L}{D_{eff} C_{max}(1-\alpha r)} = \frac{i_s L}{F D_{eff} C_{max}(1-\alpha r)} = 4\sum_{n=1}^{n=\infty}\left[\left\{\frac{\delta_n\left(\sin(\delta_n)\right)^2}{2\delta_n + \sin(2\delta_n)}\right\}e^{-\delta_n^2 \tau}\right] \tag{34}$$

$$\left(\frac{n_{Li^+,\ ini} - n_{Li^+}}{S_g L C_{max}(1-\alpha r)}\right) = 4\sum_{n=1}^{n=\infty}\left[\left(\frac{\left(\sin(\delta_n)\right)^2}{\delta_n\left(2\delta_n + \sin(2\delta_n)\right)}\right)\left(1 - e^{-\delta_n^2 \tau}\right)\right] \tag{35}$$

$$\left[\frac{I_{out,\ electrode} L}{F D_{eff} C_{max} S_g m_{electrode}}\right] = 4\sum_{n=1}^{n=\infty}\left[\left\{\frac{\delta_n\left(\sin(\delta_n)\right)^2}{2\delta_n + \sin(2\delta_n)}\right\}e^{-\delta_n^2 \tau}\right] \tag{36}$$

$$\left[\left(\frac{1}{S_g \rho_{active\ material} L}\right)\left(\frac{X_{ini} - X}{X_{max}}\right)\right] = 4\sum_{n=1}^{n=\infty}\left[\left(\frac{\left(\sin(\delta_n)\right)^2}{\delta_n\left(2\delta_n + \sin(2\delta_n)\right)}\right)\left(1 - e^{-\delta_n^2 \tau}\right)\right] \tag{37}$$

3. RESULTS AND DISCUSSION

Some typical data are presented here for the case of uniform initial distribution of lithium in the platelet-like active material particle of a cell composite electrode. The plots in Figures 2 and 3 provide insight into the transient nature of the lithium concentration $C^d(\xi,\tau)$ versus ξ profiles for two typical values of the dimensionless group, $\left(\frac{k_{eff,electro} L}{\alpha D_{eff}} = c\right)$. Comparison of these plots show the faster local depletion of lithium in the active material *via* the lithium de-intercalation process at c = 10.0 relative to that at c = 1.0. Furthermore, at each c-value for each dimensionless time group, $\tau = \frac{D_{eff} t}{L^2}$, the $C^d(\xi = 0,\tau)$ at the particle center is higher than $C^d(\xi = 1,\tau)$ at the particle surface during the period of lithium de-intercalation process.

Figures 4 and 5 show plots of dimensionless concentration, $\left[\frac{C(\xi=0,\tau) - \alpha C^b_{electro}}{C_{max}(1-\alpha r)}\right]$ and

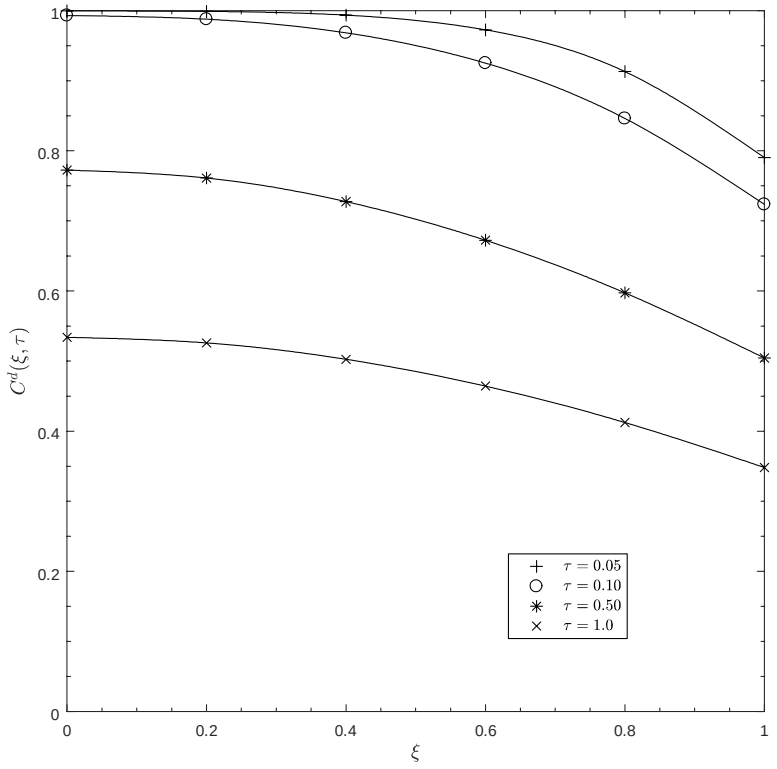

Figure 2. Plots of $C^d(\xi,\tau)$ versus ξ at c = 1.0 and at various values of τ .

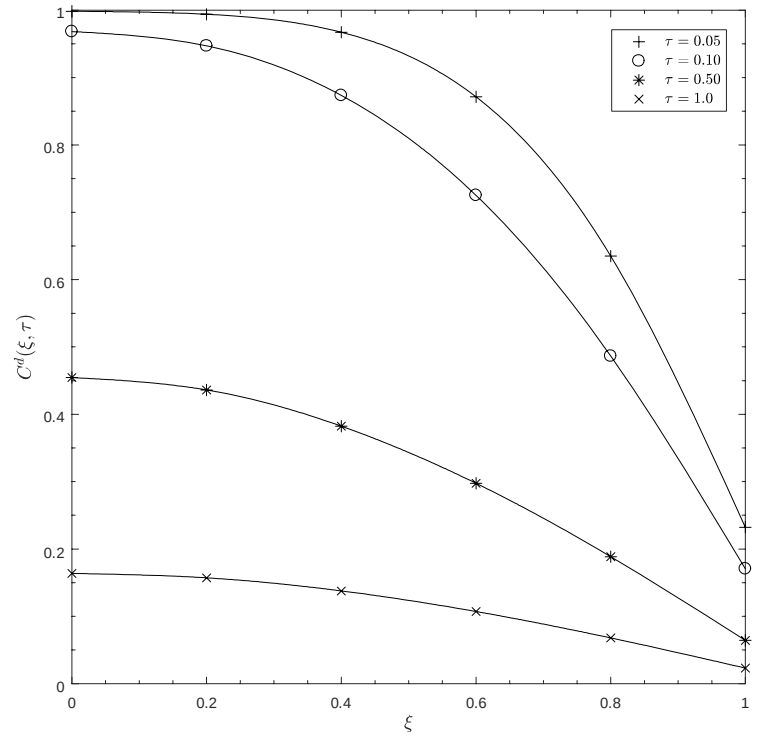

Figure 3. Plots of $C^d(\xi,\tau)$ versus ξ at c = 10.0 and at various values of τ .

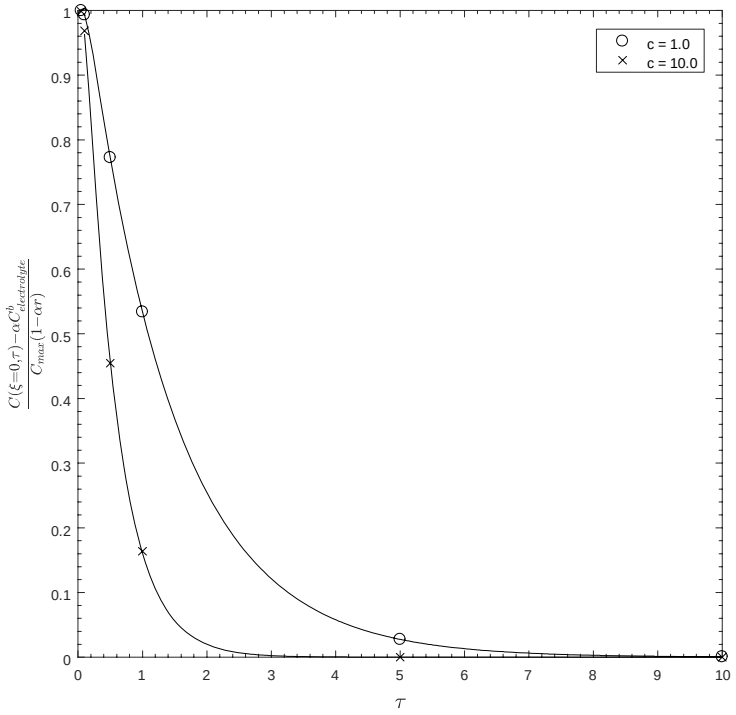

Figure 4. Transient dimensionless lithium concentration at the center of a thin platelet particle of an electrode solid active material.

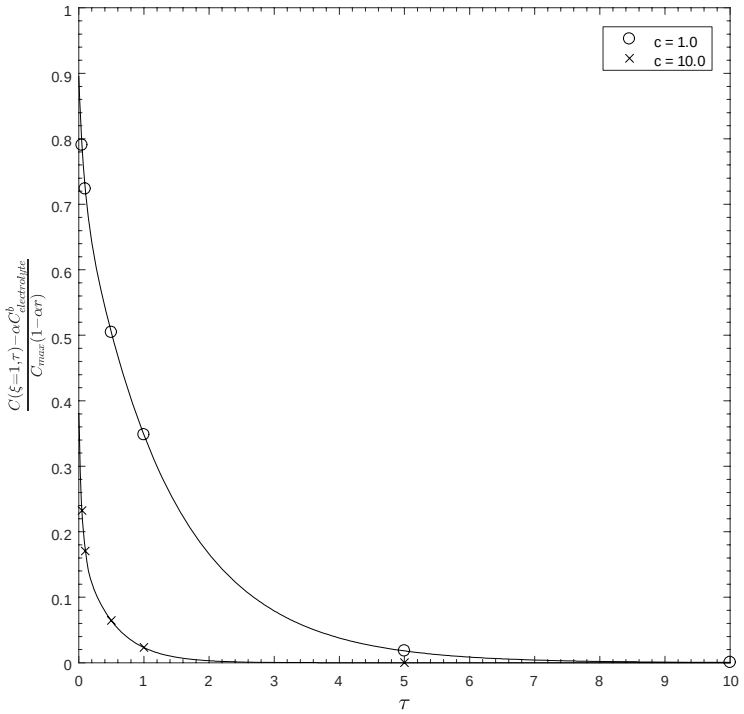

Figure 5. Transient dimensionless lithium concentration in an active material thin platelet particle at its surface in contact with an electrolyte.

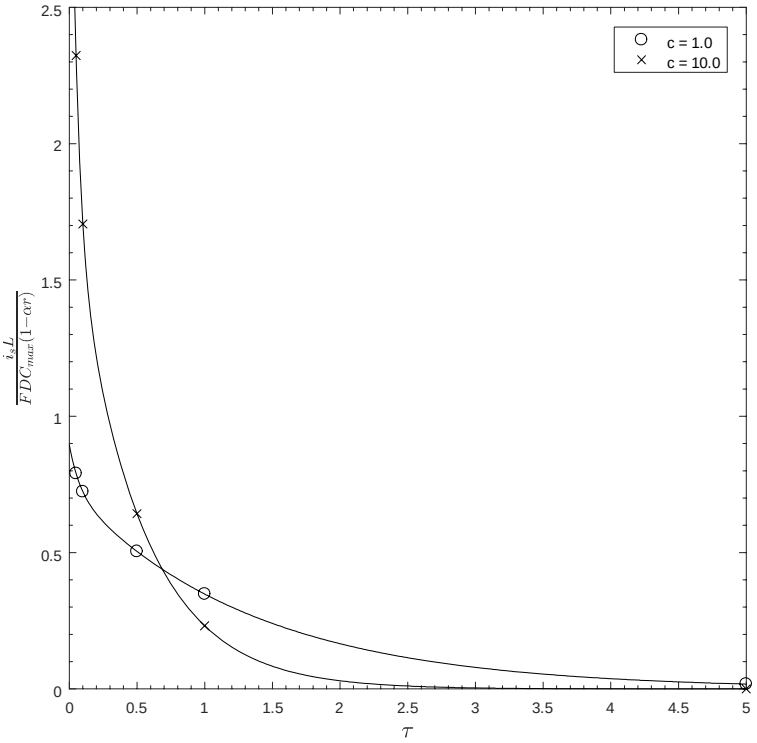

Figure 6. Transient dimensionless lithium flux or current density at the electrode active material-electrolyte interface.

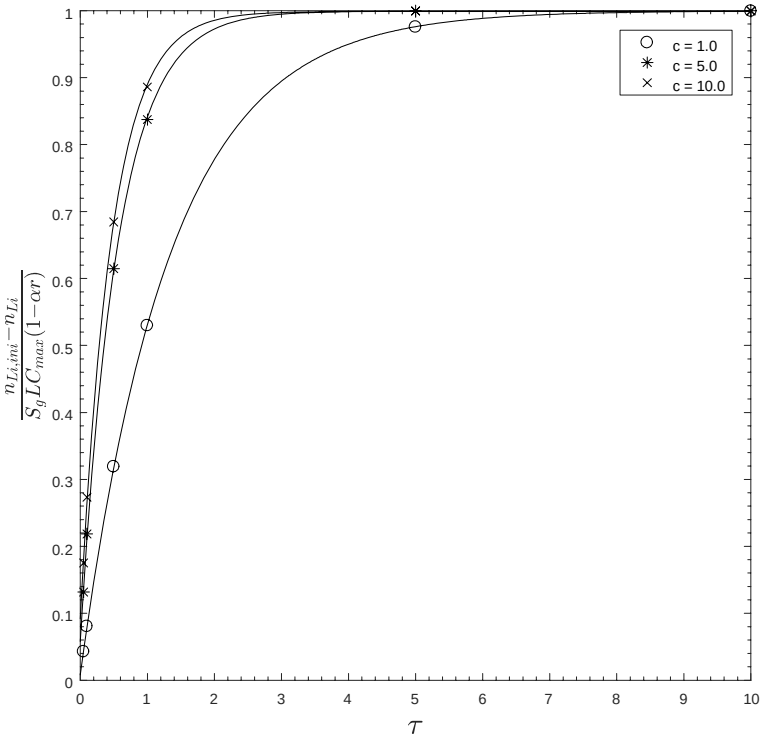

Figure 7. Transient dimensionless lithium amount extracted out of a thin platelet-like particle of an electrode active material.

$\left[\frac{C(\xi=1,\tau)-\alpha C^{b}_{electro}}{C_{max}(1-\alpha r)}\right]$ versus τ profiles, respectively, at ξ = 0 (center of the active material particle) and ξ = *1* (the particle surface) for *c* = 1.0 and 10. For each *c*-value, the dimensionless lithium ion concentrations at the particle central plane and its surface in contact with the electrolyte of a composite electrode decrease as τ increases during the period of lithium de-intercalation of the active material of an electrode. At a τ value, e.g., at τ = 1.0, the dimensionless concentrations at the active material particle central plane at ξ = 0 and at its surface at ξ = 1.0 decrease as the c-value increases as expected.

Figure 6 shows the dimensionless current-density $\left[\frac{i_s L}{FD_{eff}C_{max}(1-\alpha r)}\right]$ versus τ profiles for c =1.0 and 10.0. For each *c*-value, the dimensionless electrode active material-electrolyte interfacial current density decreases as τ increases due to the depletion of intercalatable lithium amount in the active material particle. Also, these profiles show the effect of change in *c*-values. For example, the dimensionless current density at *c* = 1.0 is less than its value at *c* = 10.0 for τ values less than 0.5. However, for τ values greater than 0.75 the dimensionless interfacial current density at *c* = 1.0 is greater than its value at c = 10.0. This is so due to the faster depletion of lithium amount in the active material particle at *c* = 10.0 than at *c* = 1.0 because of the relatively lower resistance to lithium ion mass transport in the electrolyte at the higher c value, consequently, leaving the lesser amount of lithium in the particle to provide the interfacial current density at the higher c value for τ values greater than 0.75.

Figure 7 shows the plots of the dimensionless amount of lithium extracted out of an active material particle of a composite cell electrode $\left[\frac{n_{Li,\,ini}-n_{Li}}{S_g L C_{max}(1-\alpha_r)}\right]$ as a function of τ for *c* = 1.0 and 10.0 values. It is quite obvious that the lithium amount extracted out of the active material particle increases as τ increases at each *c* value. At each τ value, the amount of lithium extracted out of the particle increases as *c* value increases in accordance with the lithium de-intercalation process controlled by the effective lithium ion mass transfer in the electrolyte relative to the effective lithium diffusion mass transfer inside the active material particle.

Analysis provided in this article for the situation of lithium ion diffusion in the cathode active material (e.g., FePc, CuPc, $LiMn_2O_4$, etc.) of a composite electrode relative to the lithium ion mass transfer in the electrolyte, affecting the electrode performance, leads to the following major conclusions.

Interfacial current density, i_s, and consequently the electrode current, $I_{out,\ electrode}$ vary as a function of time during the period of lithium de-intercalation of a composite cell electrode. Implicitly, it suggests that the lithium de-intercalation of a composite electrode should be carried out at i_s or $I_{out,\ electrode}$ as given by Eq. (34) or (36) for a given or fixed design of an electrode (i.e., for fixed values of *L*, S_g, $m_{electrode}$, C_{max} for an active material of an electrode) to keep the voltage loss associated with the charge transfer at the active material-electrolyte interface and ohmic voltage losses associated with the ion transport in the electrolyte and electron transport in the electrode at the minimum level. Operating a cell electrode at currents greater than the values predicted by Eq. (34) or (36) would result in the lower electrode performance.

The information generated on *X* versus τ from Eq. (37) can be employed to obtain the electrode reversible voltage as a function of τ from a correlation suggested in Ref. [3]. The information on the electrode reversible voltage versus time is always needed to determine the actual voltage of an operating cell of which a composite electrode is one component.

4. CONCLUSION

A theoretical model of lithium ion mass transport in a thin platelet-type active material particle relative to the lithium ion mass transport in the electrolyte was developed. This analytical model predicts the following: 1) lithium ion concentration profiles in the solid active material particle under the transient conditions, which provide insight into the nature of electrode active material lithium de-intercalation process; 2) the interfacial current

density, i_s, or total electrode current, $I_{out,\ electrode}$ as a function of time; and 3) the g-moles intercalatable lithium per g-mole of lithium-free electrode active material, X, as a function of time. Finally, the developed formulation can be used to generate the desired data on D_{eff} versus X. Subsequently, such a correlation can be used in the prediction of performance of a lithium ion cell/battery.

CONFLICT OF INTEREST STATEMENT

There are no conflicts of interest.

ABBREVIATIONS

C	molar concentration of intercalating lithium ions in the active material
$C^{b}_{electro}$	lithium ion molar concentration in bulk electrolyte
$C_{electro}\big\|_{x=L^+} = \dfrac{C\big\|_{x=L^-}}{\alpha}$	molar concentration of lithium ions in the electrolyte at $x=L^+$, $C_{electro}\big\|_{x=L^+}$ in equilibrium with the molar concentration of lithium ions in the electrode active material = $C\big\|_{x=L^-}$
$C_{Li,\ ini}$	initial molar concentration of the intercalated lithium in the electrode active material [g-mol of Li (or Li^+) $cm^{-3}_{lithium\ active\ material}$]
C_{max}	maximum intercalated lithium ion concentration in the electrode active material, such as copper phthalocyanine, and is given by $C_{max} = \left(\dfrac{\rho_{active\ material}}{M_{active\ material}} \right) X_{max}$
$\left(\dfrac{k_{eff,electro} L}{\alpha D_{eff}} \right) = c$	dimensionless group; a measure of the ratio of the lithium ion molar flux in a composite electrode electrolyte to the lithium ion molar flux in a thin platelet-like particle of a composite electrode active material
D_{eff}	effective lithium-ion mass diffusivity in a particle of a composite electrode active material
$f(x)$	the initial lithium ion dimensionless concentration distribution function
$k_{eff,\ electro}$	effective lithium ion mass transfer coefficient for lithium ion transport through the concentration boundary layer region in the electrolyte
L	half thickness of a thin, platelet-like active material particle
$m_{electrode}$	mass of the active material particles of the composite electrode free of the intercalated lithium
$M_{\ active\ material}$	molecular weight of the intercalated lithium-free active material, [gm per g-mole]
$r = \dfrac{C^{b}_{electro}}{C_{\max}}$	ratio of the bulk electrolyte lithium ion concentration to the maximum lithium ion concentration in the active material of a composite electrode
S_g	effective electrode active material-electrolyte interfacial area per unit mass of the intercalated lithium-free electrode active material
t	time coordinate
x	spatial coordinate as shown in Figure 1
X_{ini}	initial g-moles of lithium in the electrode active material per g-mole of the intercalated lithium-free active material at $\tau = 0$
X_{max}	maximum number of g-moles in the electrode active material per g-mole of the intercalated lithium-free active material
α	constant used to relate the lithium ion concentrations, $C_{electro}\big\|_{x=L^+}$ and $C\big\|_{x=L^-}$

$\xi = \frac{x}{L}$ dimensionless spatial coordinate

ρ_{active} density of active material

$\tau = \frac{D_{eff} t}{L^2}$ dimensionless time coordinate

REFERENCES

1. Tarascon, J. M. and Armand, M. 2001, Nature, 414, 359.
2. Sandhu, S. S. and Fellner, J. P. 2015, J. Chem. Eng. Process Technol., 6, 257.
3. Sandhu, S. S. and Fellner, J. P. 2013 Electrochim. Acta, 88, 495.
4. Doyle, M., Fuller, T. F. and Newman, J. 1993, J. Electrochem. Soc., 140, 1526.
5. Fuller, T. F., Doyle, M. and Newman, J. 1994, J. Electrochem. Soc., 141, 1.
6. Doyle, M., Newman, J., Gozdz, A. S., Schmutz, C. N. and Tarascon, J. M. 1996, J. Electrochem. Soc., 143, 1890.
7. Jagannathan, M. and Chandran, K. S. R. 2014, J. Power Sources, 247, 667.
8. Danilov, D., Niessen, R. A. H. and Notten, P. H. L. 2011, J. Electrochem. Soc., 158, A215.
9. Botte, G. G., Subramanian, V. R. and White, R. E. 2000, Electrochim. Acta, 45, 2595.
10. Santhanagopalan, S., Guo, Q., Ramadass, P. and White, R. E. 2006, J. Power Sources, 156, 620.
11. Ramadass, P., Haran, B., Gomadam, P. M., White, R. E. and Popov, B. N. 2004, J. Electrochem. Soc., 151, A196.
12. Guo, M., Sikha, G. and White, R. E. 2011, J. Electrochem. Soc., 158, A122.
13. Delacourt, C. and Safari, M. 2011, Electrochim. Acta, 56, 5222.
14. Renganathan, S. and White, R. E. 2011, J. Power Sources, 196, 442.
15. Ramadesigan, V., Boovaragavan, V., Pirkle, J. C. and Subramanian, V. R. 2010, J. Electrochem. Soc., 157, A854.
16. Zeng, Y., Albertus, P., Klein, R., Chaturvedi, N., Kojic, A., Bazant, M. Z. and Christensen, J. 2013, J. Electrochem. Soc., 160, A1565.
17. Bazant, M. A. 2013, Accounts of Chemical Research, 46, 1144.
18. Van der Ven, A., Bhattacharya, J. and Belak, A. A. 2013 Accounts of Chemical Research, 46, 1216.
19. Siddique, N. A., Allen, A. M., Mukherjee, P. P. and Liu, F. 2014, J. Power Sources, 245, 83.
20. Srinivasan, V. and Newman, J. 2004, J. Electrochem. Soc., 151, A1517.
21. Biesheuvel, P. M., van Soestbergen, M. and Bazant, M. Z. 2009, Electrochim. Acta, 54, 4857.
22. Safari, M. and Delacourt, C. 2011, J. Electrochem. Soc., 158, A63.
23. Bird, B. R., Stewart, W. E. and Lightfoot, E. N. 2002, Transport Phenomena, Wiley, New York, 582.
24. Spiegel, M. R. 1971, Schaum's Outline of Theory and Problems of Advanced Mathematics for Engineers and Scientists, McGraw-Hill, New York, 73, 258.
25. Spiegel, M. R. 1968, Schaum's Outline of Theory and Problems of Mathematical Handbook of Formulas and Tables, McGraw-Hill, New York.
26. Carslaw, H. S. and Jaeger, J. C. 1959, Conduction of Heat in Solids, Clarendon Press, Oxford, 491.